

Article

Continuous Fixed Bed Bioreactor for the Degradation of Textile Dyes: Phytotoxicity Assessment

Sonia Cherif ^{1,*} , Hynda Rezzaz-Yazid ¹, Salima Ayachine ¹, Imene Toukal ¹, Noredine Boudechiche ¹, Mohamed Belmedani ², Hayet Djelal ^{3,*}  and Zahra Sadaoui ¹

¹ Laboratory of Reaction Engineering, Faculty of Mechanical Engineering and Process Engineering, University of Science and Technology Houari Boumediene (USTHB), BP 32 El Alia, Algiers 16111, Algeria; yazhyn1@yahoo.fr (H.R.-Y.); salimaayachine@gmail.com (S.A.); n.boudechiche@univ-dbk.m.dz (N.B.); sadaouizahra@yahoo.fr (Z.S.)

² Laboratory of Transfer Phenomena, Faculty of Mechanical and Process Engineering, University of Science and Technology Houari Boumediene (USTHB), BP 32 El Alia, Algiers 16111, Algeria

³ UniLaSalle-Rennes, Ecole des Métiers de l'Environnement, CYCLANN, Campus de Ker Lann, 35 170 Bruz, France

* Correspondence: scherif@usthb.dz (S.C.); hayet.djelal@unilasalle.fr (H.D.)

Abstract: This study explores a novel bioremediation approach using a continuous upflow fixed bed bioreactor with date pedicels as a biosupport material. Date pedicels offer a dual advantage: providing microbial support and potentially acting as a biostimulant due to their inherent nutrients. This research is divided into two phases: with and without microbial introduction. The bioreactor's efficiency in removing two common textile dyes, RB19 and DR227, was evaluated under various conditions: fixed bed high, the effect of the initial concentration of the pollutant, and recycling the RB19 solution within the bioreactor. Optimization studies revealed an 83% removal yield of RB19 dye with an initial pollutant concentration of 100 mg·L⁻¹ using activated sludge as inoculum. The bioreactor developed its own bacterial consortium without initial inoculation. Microscopic analysis confirmed the presence of a diverse microbial community, including protozoa (*Aspidisca* and *Paramecium*), nematodes, and diatoms. The bioreactor exhibited efficient removal of RB19 across a range of initial concentrations (20–100 mg/L) with similar removal efficiencies (around 65%). Interestingly, the removal efficiency for DR227 was concentration-dependent. The bioreactor demonstrated the ability to enhance the biodegradability of treated RB19 solutions. Phytotoxicity tests using watercress and lettuce seeds revealed no negative impacts on plant growth. SEM and FTIR analyses were conducted to examine the biosupport material before and after biotreatment.

Keywords: date pedicels; fixed bed; continuous upflow; biodegradation; textile dyes; phytotoxicity



Citation: Cherif, S.; Rezzaz-Yazid, H.; Ayachine, S.; Toukal, I.; Boudechiche, N.; Belmedani, M.; Djelal, H.; Sadaoui, Z. Continuous Fixed Bed Bioreactor for the Degradation of Textile Dyes: Phytotoxicity Assessment. *Processes* **2024**, *12*, 2222. <https://doi.org/10.3390/pr12102222>

Academic Editor: Francesca Raganati

Received: 9 September 2024

Revised: 23 September 2024

Accepted: 8 October 2024

Published: 11 October 2024



Copyright: © 2024 by the authors. Licensee MDPI, Basel, Switzerland. This article is an open access article distributed under the terms and conditions of the Creative Commons Attribution (CC BY) license (<https://creativecommons.org/licenses/by/4.0/>).

1. Introduction

The impact of industrial development on the environment has led to significant consequences. Various forms of pollution, including water matrices, soil, and air pollution, are direct outcomes of industrial activities [1,2]. Among these, water pollution emerges as a paramount challenge, garnering attention from researchers worldwide [3,4]. Given the critical importance of water as a finite resource on Earth, numerous regulations have been implemented to monitor and control the quality of discharged water resulting from industrial processes.

To address this issue, various treatment techniques have been developed to mitigate and eliminate pollutants from water sources. Notably, textile dyes have emerged as a concern among the spectrum of pollutants. The textile and dyeing sector stands as the second-largest contributor to global water pollution, accounting for a significant 20% of the world's total wastewater production [5,6]. Consuming water contaminated with dyes can lead to various health issues in humans, including dermatitis, cancer, gene mutations, skin

irritation, and allergies [7,8]. Researchers are working to find strategies for their removal from water bodies, aiming to diminish their potential hazardous impact [9–11].

Numerous water decontamination techniques have been developed to address the removal of textile dye pollutants, categorized into various methods [12,13]. Physical methods encompass strategies such as adsorption, coagulation-flocculation, and others. Chemical methods, on the other hand, include photocatalysis, photo-Fenton, ozonation, and biological treatments utilizing enzymes, yeasts, fungi, bacteria, and activated sludge [14].

Despite their effectiveness, physical and chemical methods exhibit certain drawbacks, such as high cost, potential transfer of pollution from one phase to another, and the generation of substantial quantities of sludge [15]. In contrast, biological methods stand out as eco-friendly alternatives, offering a cost-effective approach to water decontamination [16–18].

Biodegradation is known as the biologically mediated breakdown of chemical molecules; it is a procedure that relies on energy and includes the decomposition of dye into different byproducts via the action of several enzymes. Different microorganisms, such as fungi, bacteria, yeasts, and algae, have been used for color removal and degradation of textile dyes [19]. It has been revealed that they have various capacities for degrading numerous dyes.

The inherent biological activities of these microorganisms enable them to enzymatically break down complex dye molecules, resulting in a more efficient and environmentally benign process compared to conventional methods [18].

Moreover, the adaptability of microorganisms to a wide range of environmental conditions further enhances their applicability in diverse textile dyeing processes. Researchers have explored the optimization of culture conditions, microbial consortia, and genetic engineering approaches to maximize the efficiency of microorganisms in dye removal [20–23].

Previous studies have demonstrated the effectiveness of fixed bed bioreactors for eliminating organic molecules [24]. This advantage can be attributed to two key factors:

Enhanced Microbial Growth: The presence of colonization support in fixed bed reactors promotes better microbial growth. Microorganisms can develop biofilms on the support, allowing them to resist environmental stresses as well as improved Mass Transfer. Fixed bed systems likely facilitate better mixing within the reactor, leading to reduced mass transfer resistance between the organic molecules and the microorganisms. This improved efficiency can contribute to enhanced degradation [24–27].

Algeria is renowned for its significant date production. However, despite this abundance, date pedicels, a byproduct of the date industry, remain largely unexplored and underutilized in our country. This untapped resource represents a substantial waste stream with potential for innovative applications. Addressing this oversight could not only mitigate environmental concerns associated with waste accumulation but also unlock new economic opportunities and contribute to the sustainable development of our agricultural sector. To fully leverage the potential of date pedicels, it is essential to understand their composition [28,29].

Date palm residues, like other lignocellulosic materials, consist of a complex array of natural compounds, including cellulose, hemicellulose, and lignin [30], along with smaller proportions of extractives and inorganic substances typically present in plant cell walls. Cellulose, also referred to as β -1-4-glucan, forms linear chains of glucose units that are densely packed and connected by hydrogen bonds, resulting in a crystalline structure. Hemicellulose, on the other hand, is a carbohydrate with an amorphous structure composed of five or six carbon sugars and functions as the adhesive that binds cellulose fibrils together. Generally, cellulose and hemicellulose collectively constitute up to two-thirds of lignocellulosic materials, representing potential sources for the production of sugars assimilated by microorganisms [31].

Lignin is the second biopolymer after cellulose; synthesized by plants, being very resistant to compression, it gives plant cells their strength. This biopolymer is mainly made up of a group of chemical substances belonging to phenolic compounds [32].

The primary objective of this study is to immobilize microorganisms on sustainable and abundant agricultural waste, specifically the discarded date pedicels in Algeria. These date pedicels will serve as consumable support for the fixed bed reactor. The novelty of our approach lies in the innovative utilization of this readily available agricultural byproduct in wastewater treatment, which, to the best of our knowledge, has not been explored as a biological support in fixed bed reactors previously.

The fixed bed reactor, incorporating microorganisms immobilized on dates' pedicels, will be applied for the removal of two textile dyes: Reactive Bleu 19 (RB19) and Direct Red 227 (DR227). To assess the efficacy of this system, biodegradability and phytotoxicity tests will be employed to evaluate the treated solutions' quality. This pioneering study aims not only to address the environmental challenge of textile dye removal but also to introduce a sustainable and novel application of date pedicels as a biological support in fixed bed reactors.

2. Materials and Methods

2.1. Textile Dyes

Two textile dyes, Reactive Blue 19 (RB19) and Red Direct 227 (DR227), were selected for this study due to their widespread use and persistence in the environment. RB19 is a highly harmful textile dye with strong biological stability and resistance to conventional chemical and photocatalytic processes; its maximum wavelength is 590 nm, it was purchased from ACROS Organics. DR227 is a bi-azo dye known for its high stability; its maximum wavelength is 545 nm, it was obtained from the TEXALG textile industry located in Boufarik, Blida, Algeria. Figure 1 illustrates the molecular structures of these two dyes [33].

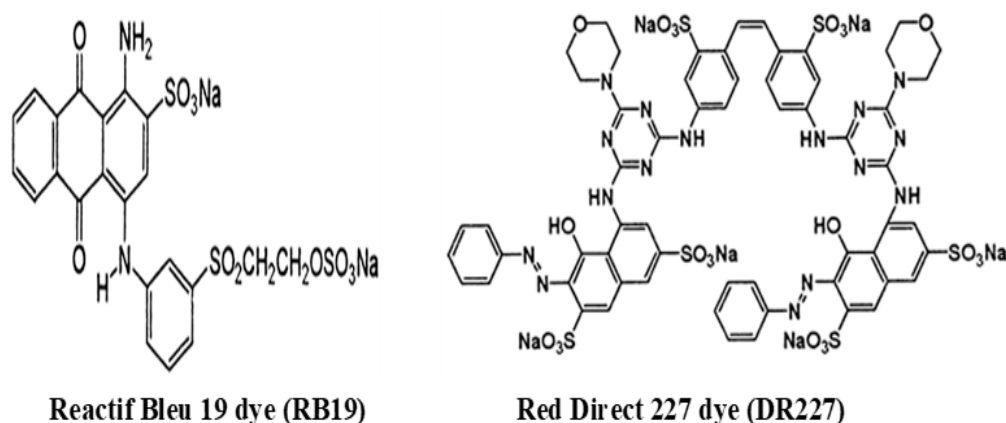


Figure 1. Molecular structure of the targeted dyes.

The main characteristics of the two dyes are presented in our previous study [33]. The molecular structure of the target molecules is illustrated in Figure 1.

All the dye solutions were prepared with tap water. The biological support is composed of date pedicels and activated sludge.

2.2. Date Pedicels

The date pedicels were first washed to remove any dust or impurities and then allowed to dry. Once they were dry, the stems were cut into small pieces approximately 1 cm in length [28].

2.3. Activated Sludge

The activated sludge samples were collected at the outlet of the aeration basin of the Réghaia water treatment plant, Algiers, in a polyethylene container. Then, they were placed in a cooler and transported to the laboratory. Upon arrival, they were immediately stored at 4 °C in a refrigerator until further use.

2.4. Operating Mode

In pursuit of transitioning towards continuous operation, we engineered a fixed bed bioreactor to facilitate the process of continuous upflow. The setup integrated a supply tank linked to a peristaltic pump (ISMATEC) responsible for delivering a continuous upward flow (0.3 L/h) into the column, which had a diameter of 3 cm and a height of 50 cm for column 1 and 170 cm for column 2. The height of the fixed bed was 36 cm for column 1 and 106.5 cm for column 2. Within the column, a specialized biological support matrix was meticulously packed. To ensure optimal oxygenation of the culture medium, air was introduced from the column's base, facilitated by an aquarium aerator (NB-8002B with one outlet for column 1 and PYPABL with four outlets for column 2). Inert stones were introduced at the bottom of the column to prevent the water and air pipes from being blocked by pieces of date pedicels. Provision was made for sampling outlets to facilitate monitoring and analysis throughout the process.

The schematic representation of the experimental setup for the continuous biological degradation of two textile dyes is visually depicted in Figure 2.

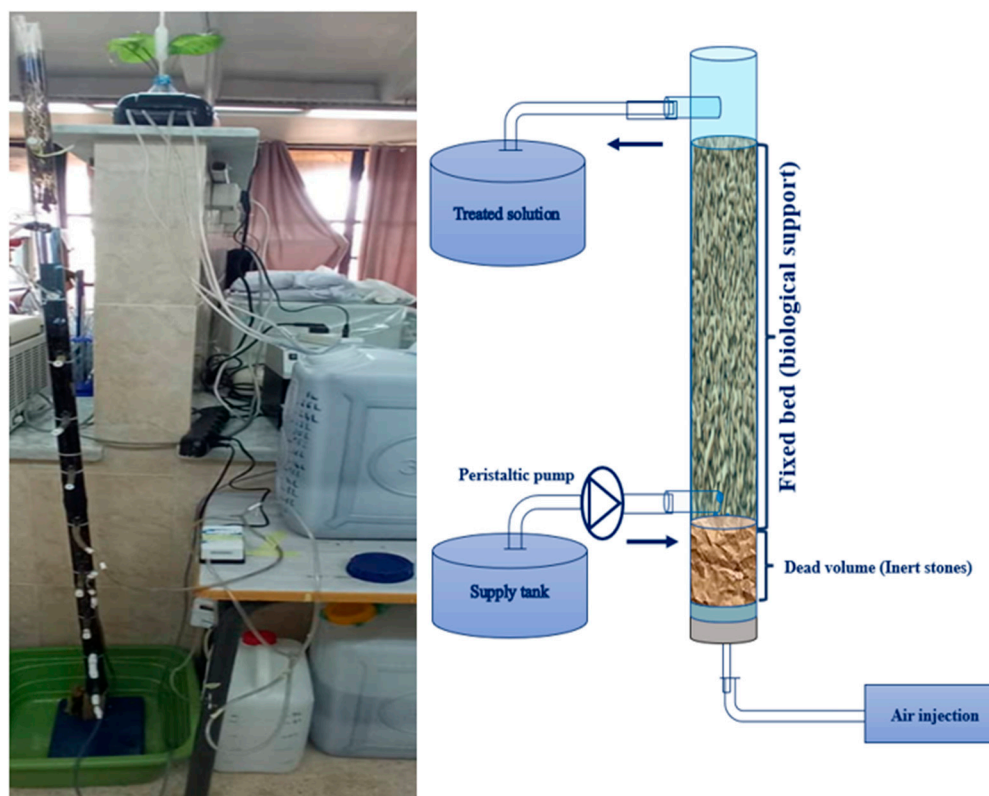


Figure 2. Experimental device of the fixed bed bioreactor.

The samples taken before and after treatment were centrifuged at a speed of 7000 rpm for 10 min before being analyzed. The absorbances (590 and 545 nm for RB19 and DR227, respectively) were determined by UV/Visible spectrophotometry (OPTIZEN 2120UV, Mecasys Co., Ltd., Daejeon, Republic of Korea).

The degradation efficiency of the mixture of the two dyes was determined using the following formula based on the change in maximum absorbance:

$$\text{Degradation yield (\%)} = \left(\frac{C_0 - C_f}{C_0} \right) \times 100$$

C_0 : Initial concentration at the entrance to the column.

C_f : Concentration at the outlet of the column at time t .

To optimize the degradation yield, several parameters were investigated, including the effect of biological treatment with and without seeding, the height of the fixed bed bioreactor, pollutant concentration, dye degradation cycle, and dye type.

The experiments were conducted in duplicate to ensure the reproducibility of the results. The amount of date pedicels used in this study was 108.5 g in column 1 and 318 g in column 2.

2.5. Seeding the Culture Medium

The seeding of the culture medium was carried out by adding the activated sludge (2 L) without any pretreatment that contains the microorganism's consortium to the date pedicels. The inoculum was recirculated in the column for 3 h in loop mode to ensure good fixation of the microorganisms on the date pedicels with a flow rate of $0.3 \text{ L} \cdot \text{h}^{-1}$. Then, the biodegradation experiments of the RB19 dye were initiated. Some of the microorganisms attached to the biological support, while those that did not were discharged in the outlet effluent.

2.6. Analytical Methods

2.6.1. Biological Oxygen Demand (BOD₅)

The BOD was measured after 5 days (BOD₅), at 20 °C (temperature favorable to the activity of O₂-consuming microorganisms), and in the dark (in order to avoid any parasitic photosynthesis) [34].

The sample to be analyzed was introduced into the Oxitop device. The device was equipped with a nutrient medium, a buffer solution, a nitrate inhibitor solution, and activated sludge. The pH of the solution was adjusted to 7.0 ± 0.2 using either 0.01 M H₂SO₄ or 0.01 M NaOH.

NaOH was placed in the rubber cap of the BOD₅ bottle. After a period of 5 days, BOD₅ measurements were recorded. The values obtained were multiplied by the dilution factor to obtain the final BOD₅ value.

2.6.2. Chemical Oxygen Demand (COD)

Water quality was assessed using the Chemical Oxygen Demand (COD) method, which indicates the degree of organic pollution removal. COD levels were measured using a Hanna HI93754A-25GB COD analyzer (Hanna Instruments, Nusfalau, Romania). In this process, a 2.5 mL sample was added to multiple tubes containing the Ag₂SO₄/H₂SO₄/K₂Cr₂O₇ mixture and heated to 150 °C for 2 h [35].

2.6.3. Phytotoxicity of Germination Tests on Watercress and Lettuce Seeds

Ten filter papers were placed into ten Petri dishes and then moistened with 5 mL of the sample to be analyzed. The tests were conducted using two types of seeds: watercress and lettuce. Each Petri dish was seeded with 10 watercress or lettuce seeds. Subsequently, all Petri dishes were incubated in an incubator set at a temperature of 25 °C for a period of 48 h.

Under identical conditions, a control sample was prepared using ten Petri dishes, each containing 5 mL of tap water and ten watercress or lettuce seeds [33].

The germination index (GI) was calculated by averaging the number of germinated seeds and the average length of the roots, as determined by the following formula:

$$\text{GI (\%)} = \left(\frac{\text{seedgermination(\%)} \times \text{averagerootlengthofthesample}}{\text{seedgermination(\%)} \times \text{averagerootlengthofthecontrol}} \right) \times 100$$

2.6.4. Visualization by Microscope

This section focuses on the second part of the study, which examines biodegradation without inoculating the medium with microorganisms. The aim was to assess whether the bioreactor could naturally develop a microbial community capable of degrading the

dye, particularly after observing suspended particles in the treated solution. To better understand the nature of these particles, observations were conducted using an inverted microscope (Optika, Ponteranica, Italy) at a magnification of $40\times$.

The purpose of this observation was to identify the presence of microbial or non-microbial particles that could be contributing to the degradation process. The samples were observed in their natural state, without the addition of reagents or staining protocols, highlighting one of the advantages of using the inverted microscope. This approach allowed for the real-time observation of particle morphology and behavior, preserving the integrity of the samples and ensuring a more accurate representation of the system's dynamics.

2.6.5. Characterization of the Biological Support

FTIR and SEM analyses were performed on the date pedicels both before and after the biodegradation process. After biodegradation, the biological support material was dried at ambient temperature for 48 h before analysis. The primary purpose of this characterization was to examine any structural or chemical changes that may have occurred in the biological support during the biodegradation process.

Scanning Electron Microscopy (SEM) was used to observe the microscopic morphology of the date pedicels before and after biodegradation. The analysis was conducted using a Quanta 250 SEM (FEI Company, Eindhoven, The Netherlands) equipped with a tungsten filament. In addition, Fourier-Transform Infrared (FTIR) spectroscopy was employed to identify functional group changes in the material. FTIR spectra were recorded using a BRUKER spectrophotometer (Bruker, Ettlingen, Germany), covering a wavelength range of $400\text{--}4000\text{ cm}^{-1}$.

3. Results and Discussion

3.1. Biological Treatment with Seeding

3.1.1. Fixed Bed Height

The fixed bed is generally a material that has a large specific surface area on which bacteria attach. As the dye flows through the fixed bed, the structural composition of the material facilitates the effective mixing of the effluent by introducing air, thereby optimizing the process.

The effectiveness of the elimination process depends on several factors, including the height of the bacterial bed. Indeed, the increase in the height of the biomass bed means the amplification of the bacterial population residing there. The biological degradation of RB19 in a fixed bed was carried out by adopting two heights of the biological support: 106.5 cm and 36 cm.

Figure 3a shows the effect of the biological support on degradation efficiency, while Figure 3b illustrates the impact of fixed bed height on pH variation. The evolution of the degradation efficiency of the RB19 dye, presented in Figure 3a, shows two phases. The first phase is characterized by a significant increase in yield during the first three days of treatment, reflecting a progressive adaptation of the microorganisms to the operating conditions of the reactor. During the second phase, the removal efficiency of RB19 stabilizes around 70% and 51% for bed heights of 106.5 cm and 36 cm, respectively. These results demonstrate a clear correlation between bed height and discoloration efficiency. Discoloration efficiency increased from 51% to 70% as the bed height increased from 36 cm to 106.5 cm, respectively.

Date pedicels, being rich in carbon as an energy source, provide a favorable environment for microbial development [36]. Additionally, essential nutrients like nitrogen, phosphorus, and mineral ions are necessary to support various metabolic processes. Microorganisms in activated sludge utilize these organic materials and inorganic nutrients for their growth and maintenance. This microbial activity ultimately leads to the degradation of the target molecule of interest.

After passing through the biological stage (fixed bed), the treated effluent undergoes centrifugation to separate the purified dye solution from excess bacteria that may have detached from the fixed bed during the treatment process.

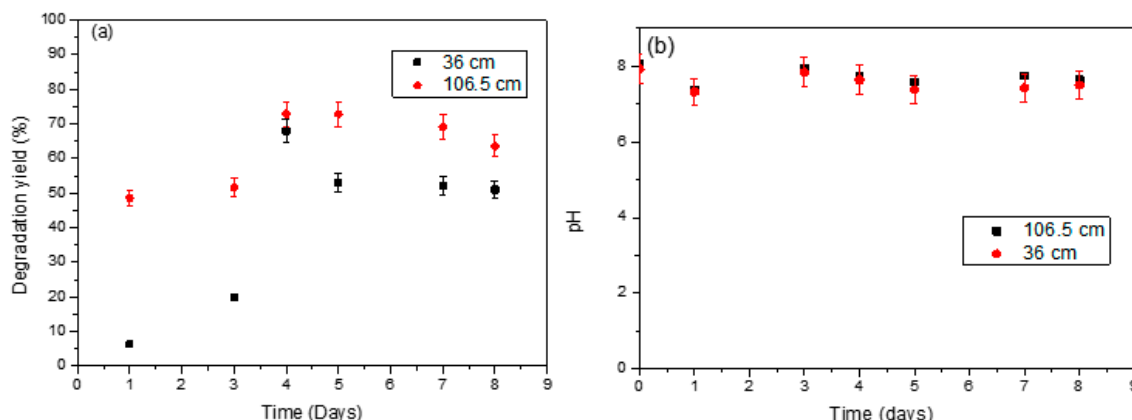


Figure 3. Effect of biological support height on (a) degradation yield of RB19 dye; (b) pH variation (free pH = 7.97; initial C = 5 mg·L⁻¹; flow rate: 0.3 L·h⁻¹).

The fixed bed bioreactor with date pedicels employs a combination of physical, chemical, and biological processes to achieve biodegradation of textile dyes. The degradation mechanism focuses on diffusional flux, mass transfer, and bioreaction:

Date pedicels serve as a biosupport, providing a surface for microbial attachment and biofilm formation. As wastewater containing target dyes (RB19 and DR227) flows through the bioreactor, a concentration gradient drives the diffusion of these dissolved dye molecules through the biofilm.

The rate of diffusion is influenced by the biofilm's structural characteristics, including thickness, density, and the presence of extracellular polymeric substances (EPS) produced by the microbial community. These factors can significantly impact the accessibility of dye molecules to the microorganisms residing within the biofilm [37,38]. Once through the biofilm, the dye molecules reach the mass transfer zone, located at the interface between the biofilm and the bulk liquid. Here, mass transfer processes govern the movement of dye molecules from the bulk liquid to the microbial cells within the biofilm. Factors like flow rate, turbulence within the bioreactor, and biofilm thickness all influence the efficiency of mass transfer [39,40].

The key players in the biodegradation process are the diverse microbial populations attached to the date pedicels. These microorganisms possess enzymatic machinery specifically designed to break down complex dye molecules into simpler compounds [41].

The specific enzymatic capabilities of different microbial species determine their roles in the degradation pathway. Some microbes might be adept at initial decolorization, while others specialize in further mineralization of the breakdown products [42]. The presence of date pedicels as a potential biostimulant could enhance this process. Nutrients present within the dates might support microbial growth and activity. Additionally, the percentage of cellulose, hemicellulose, and total sugar in the date pedicels is important. Consequently, the presence of assimilable sugars resulting from their hydrolysis can promote the development of microorganisms responsible for the biological degradation of the dyes, leading to improved biodegradation efficiency [36].

Following biodegradation by microorganisms, the resulting simpler compounds or mineralized products are released back into the bulk liquid. Biodegradation is likely not a single, linear pathway. Complex dyes might undergo sequential enzymatic breakdown by different microbial populations within the biofilm [43].

Enayatzamir et al. (2009) investigated the potential of *Trametes pubescens* for the decolorization of the recalcitrant diazo dye, Reactive Black 5 (RB5). Their study employed the white-rot fungus immobilized on stainless steel sponges within a fixed bed reactor for laccase production and subsequent dye decolorization. Notably, they achieved a maximum RB5 decolorization rate of 74% within a 24 h period. The authors attributed the decolorization process to two primary mechanisms: dye adsorption, adsorption of RB5

molecules onto the mycelial network of the fungus, and laccase-mediated degradation, enzymatic breakdown of the dye by laccase enzymes produced by *Trametes pubescens* [44].

In our work, suspended solids increased at some point during processing and then decreased. This can probably be explained by the detachment of biofilm fragments. The same remark was noted by El Jaafari et al. (2017) [45].

Throughout the experiments, the pH remained close to neutral (Figure 3b).

3.1.2. The Concentration of the Pollutant

This section addresses the impact of pollutant concentration on the biodegradation process. Figure 4 illustrates the effect of the initial concentration of RB19 on the degradation rate over time (a), pH variation (b), and conductivity variation (c) under experimental conditions.

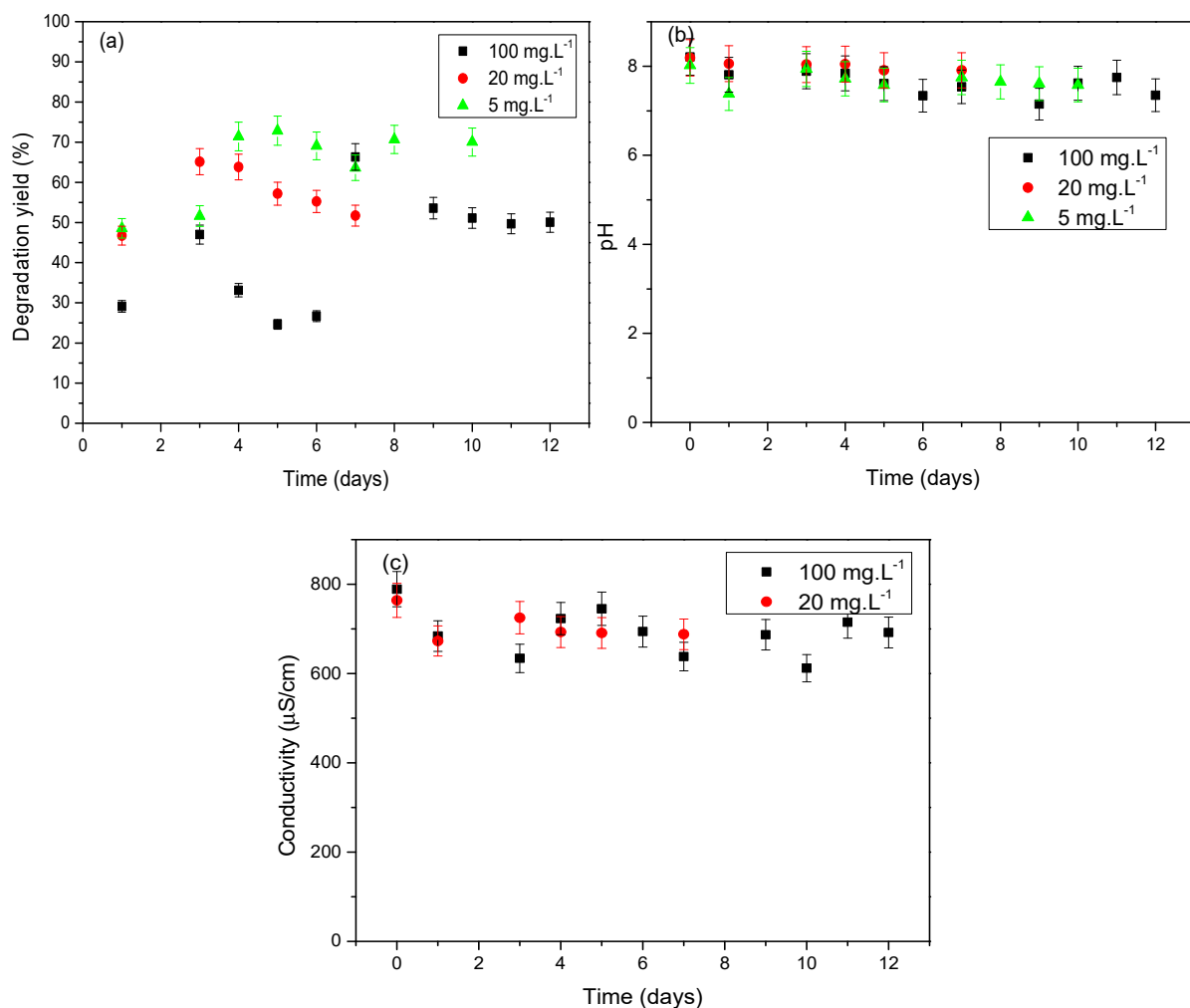


Figure 4. Effect of the initial concentration of RB19 on (a) yield of degradation: (b) variation of pH, (c) variation of conductivity (pH (5 mg L⁻¹) = 7.97; pH (20 mg L⁻¹) = 8.19; pH (100 mg L⁻¹) = 8; fixed bed height = 106.5 cm; flow rate: 0.3 L·h⁻¹).

The effect of the initial RB19 concentration on the biodegradation kinetics was investigated using three different concentrations: 5, 20, and 100 mg·L⁻¹. Interestingly, the results showed similar color removal efficiencies (around 65%) for the two higher concentrations (20 and 100 mg·L⁻¹).

These findings suggest that the biological treatment process remained relatively constant within this concentration range (20–100 mg·L⁻¹). This observation aligns with the work of Cherif et al. (2021), who reported a consistent removal efficiency of around 70% for

RB19 dye at concentrations ranging from 100 to 2500 mg/L during their biodegradation by biostimulation study [28].

A daily pH measurement was carried out for all the concentrations studied, which shows that all values remain close to neutrality (Figure 4b). In fact, date pedicels have a buffering power, maintaining the pH close to neutrality, whatever the initial pH of the solution to be treated. Similar results were obtained by Cherif et al. (2021) during the biological treatment of textile dye RB19 in batch mode using date stems as a co-substrate. The pH remains close to neutral regardless of the initial pH of the sample [28].

Daily measurements of the treated solution's conductivity revealed a variation range between 500 μS and 700 μS (Figure 4c). This increase in conductivity compared to the initial value suggests the release of ions into the solution. These ions could potentially originate from two sources. Decomposition Products: The breakdown of the RB19 molecule itself might release charged ions as byproducts of the degradation process. Mineral Salts from Date Pedicels: The date palm pedicels used as a carrier material may leach out mineral salts during the treatment process, contributing to the observed conductivity increase.

3.1.3. Recycling

To further increase the color reduction yield, the final solution, treated biologically at an initial concentration of 100 $\text{mg}\cdot\text{L}^{-1}$, was recycled twice through the fixed bed bioreactor. In this context, Figure 5 presents (a) the degradation yield of RB19 dye during the recycling of the treated solution, (b) the evolution of pH during the recycling process, and (c) the variation in conductivity during the recycling of the treated solutions under experimental conditions.

Recycling the RB19-treated solution through the bioreactor significantly enhanced biodegradation efficiency. As illustrated in Figure 5a, recycling solution 1 initially displayed a rising biodegradation yield, reaching a peak of 55% within the first three days. However, the yield subsequently decreased in the following days. A similar trend was observed with recycling solution 2, with an initial increase to 35% followed by a decline.

Overall, recycling the RB19 solution twice through the bioreactor led to an approximately 40% increase in biodegradation rate, ultimately achieving a total removal efficiency of 83%. This improvement can be attributed primarily to an extended substrate-biomass contact time. During the first cycle, the residence time within the bioreactor might not have been sufficient for optimal transfer of the RB19 solution from the bulk liquid to the microbial biomass on the date pedicels [39].

The observed decrease in removal efficiency after the initial rise could be due to two potential reasons. Competitive Byproducts: The decrease in removal efficiency compared to the first operating cycle may be due to the presence of intermediate organic molecules that appeared during the first RB19 degradation cycle. These molecules are probably more recalcitrant than RB19, and are therefore competitive, which significantly affects the degradation of the target pollutant.

Pressure Limitations: The growth and activity of microorganisms within the column could have led to increased pressure within the system. This pressure buildup might have hindered airflow through the column, thereby limiting oxygen supply and reducing pollutant degradation efficiency.

To address these potential limitations, subsequent experiments employed a fixed bed column with a reduced height of 36 cm. This shorter column design facilitates air flow and minimizes pressure losses, ensuring optimal oxygen availability for microbial activity throughout the bioreactor.

Consistent near-neutral pH values were observed across all trials (Figure 5b), while conductivity varied between 550 μS and 790 μS (Figure 5c).

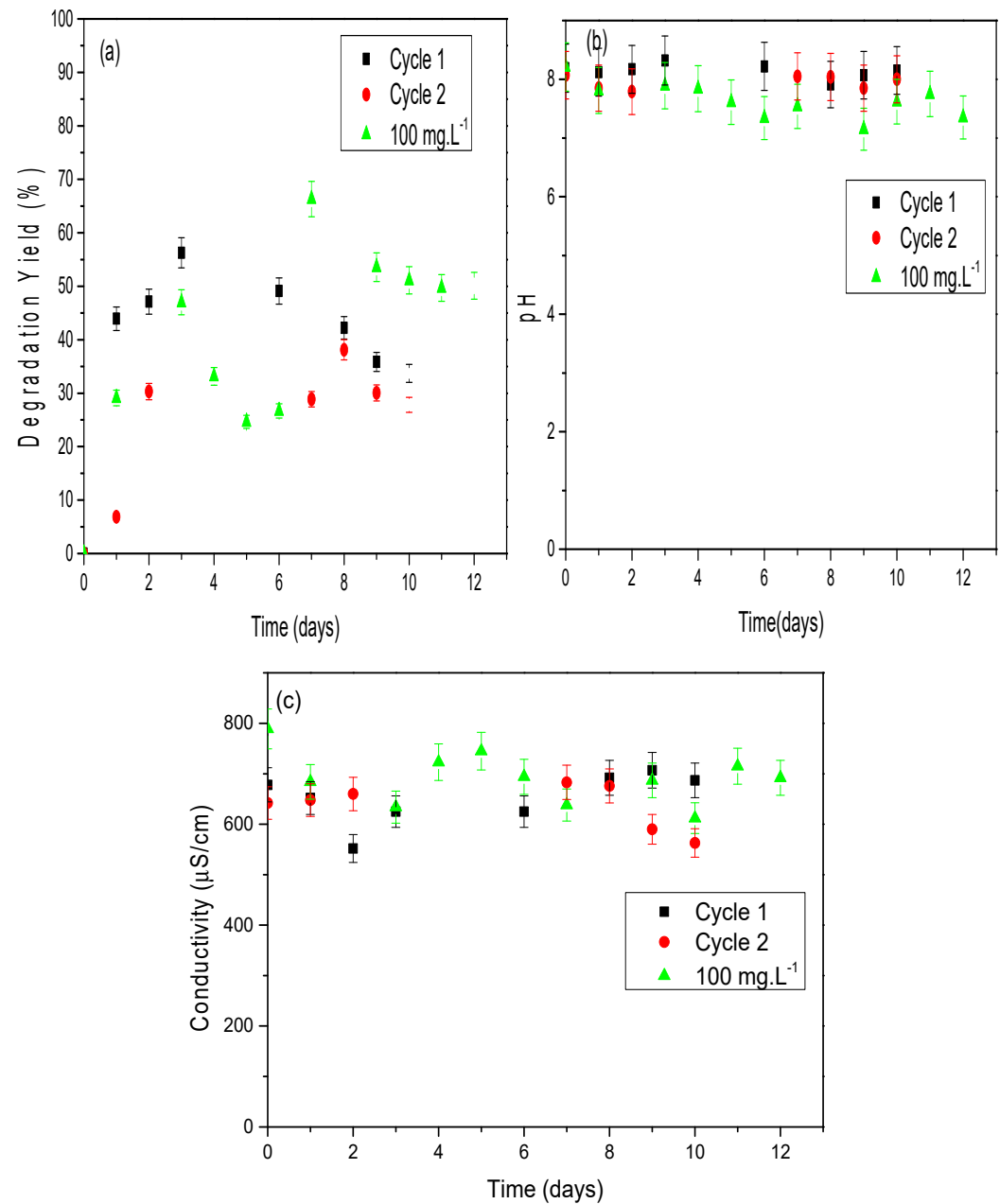


Figure 5. (a) Evolution of the degradation yield of RB19 during the recycling of treated solutions, (b) evolution of the pH during the recycling of the treated solutions, and (c) evolution of conductivity during recycling of treated solutions (pH (100 mg.L⁻¹) = 8; pH_{cycle1} = 8.23; pH_{cycle2} = 8.15; fixed bed height = 106.5 cm; flow rate: 0.3 L.h⁻¹).

3.2. Biological Treatment without Seeding

The activated sludge process operates on the fundamental principle that wastewater, when aerated, fosters the gradual development of a bacterial community, which actively competes against and breaks down the harmful organic pollutants present [46].

In this context, we used the column filled with date stems with a height of 36 cm in order to examine a possible development of microorganisms around our biological support (without inoculum). The parameters to study in this part are initial dye concentration and dye type.

3.2.1. The Concentration of the Pollutant

According to previous studies, increasing the concentration of dye can gradually decrease the biodegradation rate, which is likely due to a toxic effect on the bacteria [47]. To investigate this effect, the RB19 removal efficiency was evaluated in the unseeded column using two concentrations: 5 mg/L and 20 mg/L. Accordingly, Figure 6 illustrates (a) the impact of the initial RB19 concentration with and without seeding, (b) the effect of the initial dye concentration on degradation, (c) pH variation, and (d) conductivity variation under experimental conditions.

The comparison of the performance of the fixed bed column with and without seeding for the 5 mg/L RB19 concentration shows that the removal efficiency was relatively low (30–40%) during the first seven days (Figure 6a). This initial period likely corresponds to the microorganisms' adaptation to the new environment. Following this adaptation phase, the biological efficiency increased to 60%. This observation suggests a rapid development of the bacterial population after 13 days, indicating their successful degradation of the pollutant.

These findings highlight the advantages of using date pedicels as a consumable carrier material with fixed biomass. The nutrients and total sugars present in this biostimulant likely promote the rapid proliferation of the bacterial community, which is further enhanced by other factors such as aeration and the readily available carbonaceous material within the pollutant itself.

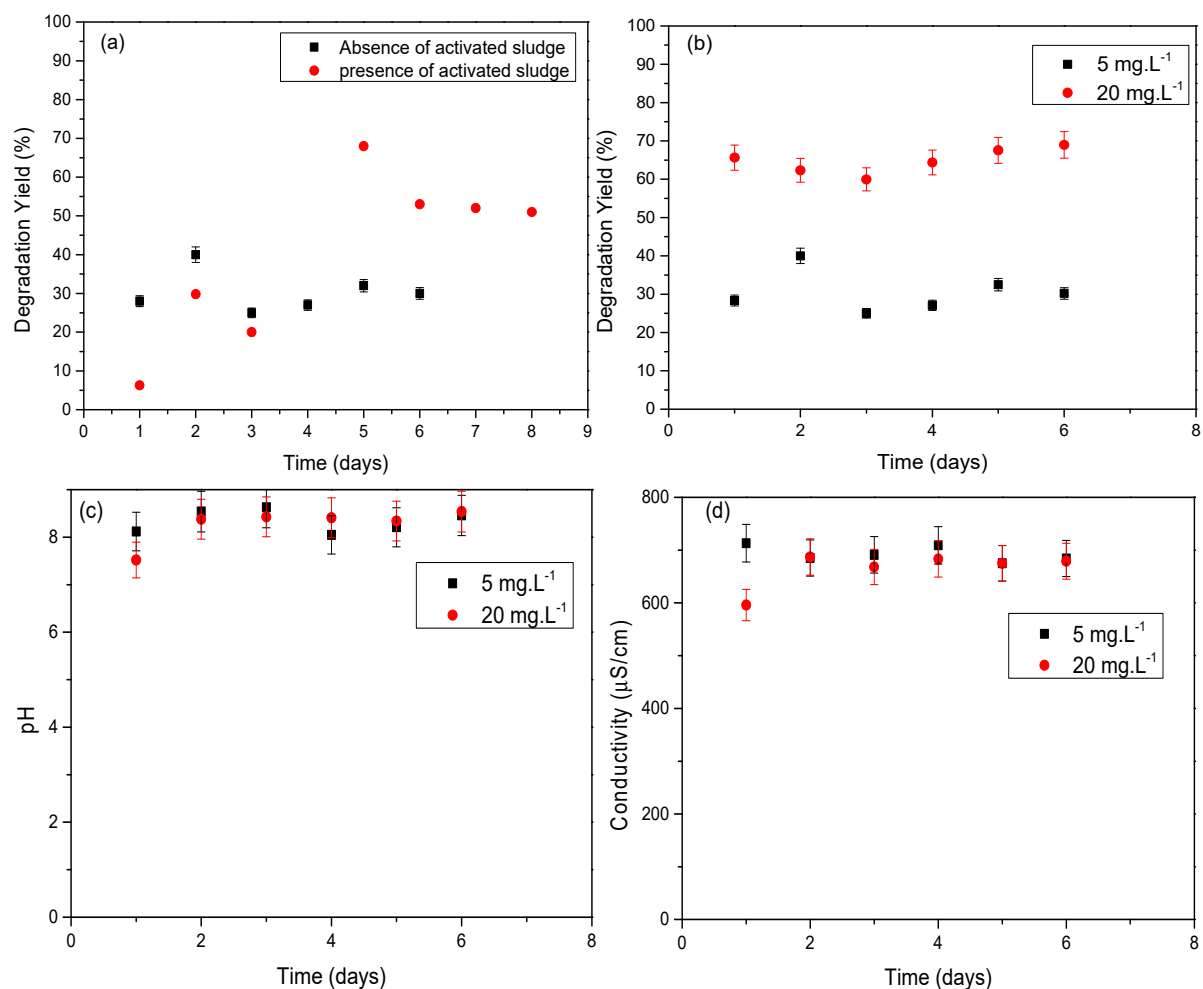


Figure 6. Effect of initial concentration of RB19. (a) Evolution of the biodegradation yield of 5 mg·L⁻¹ of RB19 molecule with and without seeding. (b) Effect of the initial concentration of the dye. (c) Variation of pH. (d) Variation of conductivity. (pH (5 mg·L⁻¹) = 8.2; pH (20 mg·L⁻¹) = 7.92; fixed bed height = 36 cm; flow rate: 0.3 L·h⁻¹.).

We also notice that there is a slight difference between the column removal efficiency with seeding (70%) and without seeding (60%), which proves the capacity of the biomass produced to degrade recalcitrant organic matter.

Figure 6b shows that the elimination efficiency of the RB19 molecule with an initial concentration of $20 \text{ mg} \cdot \text{L}^{-1}$ is greater than that of $5 \text{ mg} \cdot \text{L}^{-1}$; this is probably due to the phase of adaptation of the dye to the environment and the development of the microorganisms community, which took around ten days; once it adapted, it gave better results even with a higher concentration.

Mohanty et al. (2021) targeted the eco-friendly removal of Indanthrene Blue RS dye using a microbial consortium immobilized on corn-cob biochar in a continuous upflow packed bed bioreactor. The maximum biodegradation rate achieved was 90% at a concentration of 500 mg/L. Beyond this concentration, the decolorization rate decreased [48].

There were minimal fluctuations in pH, which remained close to neutral during all experiments (Figure 6c). In contrast, conductivity varied between 600 μS and 700 μS (Figure 6d).

3.2.2. Observation by Inverted Microscope

During the degradation of the RB19 dye without seeding, we noticed the presence of a sludge that settled at the bottom of the test tube with each sample. The analysis and identification of this sludge formed proved useful for obtaining maximum information on the composition of the latter, as well as the quality of purified water and toxicity.

Microfauna is made up of microscopic animals called protozoa and metazoa. These organisms participate in the elimination of free bacteria that constitute their prey and in the cohesion of the floc through their droppings. Their observation under a microscope provides indications on the quality of the treatment and can quickly reveal possible operating anomalies [49].

In this context, we utilized an inverted microscope to observe the microbial consortium, allowing us to visualize various species without the need for traditional staining protocols (Figure 7). Figure 7 presents (a) an overall image of the microbial consortium, (b and c) photographs of *Paramecium*, (d) a photograph of Nematodes, (e) a depiction of flocculated growth, and (f) an image of dispersed growth.

Microbial communities within activated sludge exhibit diverse growth morphologies. These can be broadly categorized into three main types: flocculated growth, dispersed growth, and filamentous growth. Within a functional activated sludge system, all three forms coexist. However, for optimal performance, flocculated growth is the most desirable. Flocculated bacteria readily aggregate into larger structures called flocs, which settle more efficiently during clarification. This efficient settling facilitates the separation of treated water from the activated sludge biomass in the clarifier, ultimately ensuring good quality of the discharged effluent [50]. As visualized through microscopy (Figure 7), all three growth morphologies are present in the system, with a clear predominance of flocculated growth. Several species that usually exist in activated sludge have been observed.

For metazoans, there were mainly nematodes, which are mobile organisms with a smooth wall; they are quite resistant to under-aeration of the environment. Their presence is not unfavorable to the purifying process. The presence of intestinal nematodes, particularly *Ascaris* sp., in wastewater is considered a major risk for health and for the reuse of this water in agriculture [51]. Concerning the protozoa, we note the presence of *Aspidisca* and *Paramecium* belonging to the ciliates family. Their presence indicates good water quality; they are resistant to periods of anoxia or aeration shutdown [50]. We also note the presence of microalgae type *Diatom*, which may originate from date pedicels. *Diatoms* are recognized for their purifying power of wastewater [52].

This diverse ecosystem indicates favorable conditions for biodegradation processes within the bioreactor and highlights the system's ability to establish a diverse microbial community capable of degrading textile dyes, although further research might be needed to optimize the development of this indigenous consortium.

The presence of detached fragments of the biofilm in the treated solution could pose a problem. Therefore, we suggest measuring the microbial cell density at both the inlet and outlet of the bioreactor. Additionally, implementing sand filtration at the outlet can help refine the treatment process and retain these detached biofilm fragments.

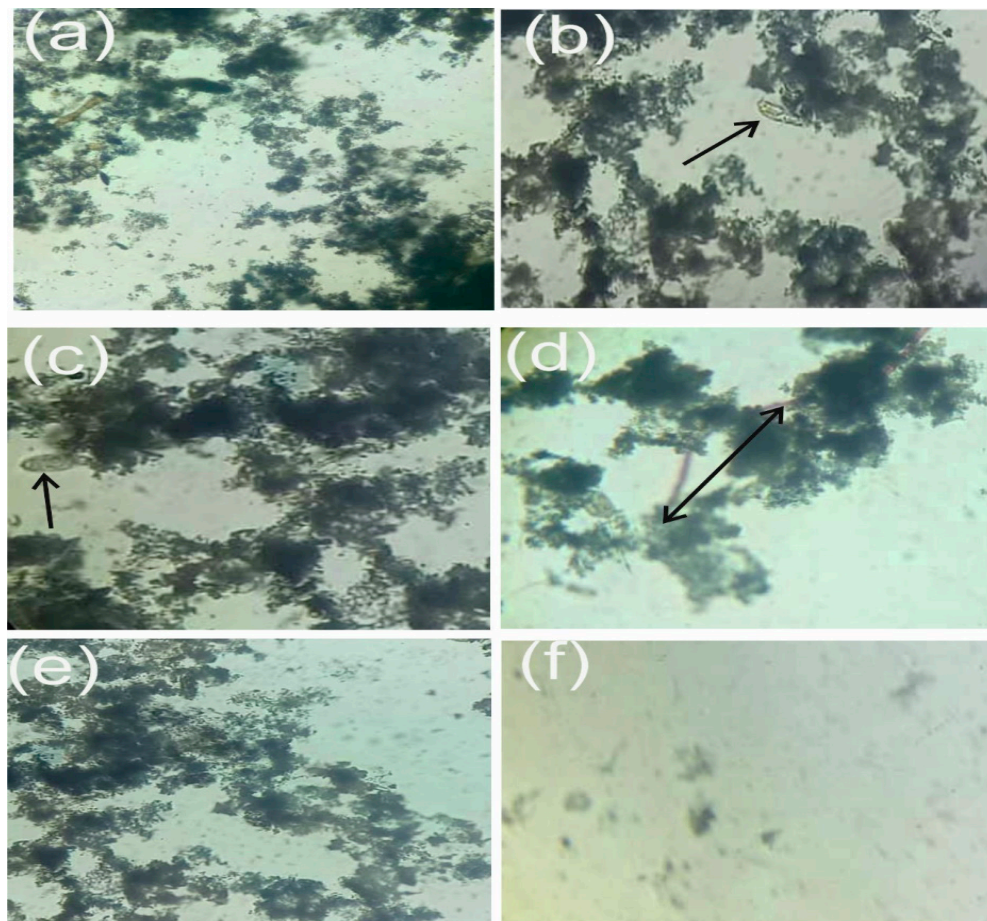


Figure 7. Observation by inverted microscope (40×) (a) global image, (b,c) *Paramecium*, (d) Nematodes, (e) flocculated growth, (f) dispersed growth (final solution without seeding) (pH = 7.97; RB19 concentration = 20 mg·L⁻¹; fixed bed height = 36 cm).

3.2.3. The Type of Dye

In order to examine the effectiveness of the fixed biomass column on other types of textile dyes, another study was conducted on the dye DR227, using two concentrations: 5 and 20 mg/L. Figure 8 depicts the impact of the initial concentration of DR227 on the degradation rate (a), pH variation (b), and conductivity variation (c) under experimental conditions.

The biodegradation efficiency of DR227 dye was concentration dependent. At an initial concentration of 5 mg/L, the purification efficiency reached around 50%. However, this efficiency decreased to approximately 30% for an initial concentration of 20 mg·L⁻¹ (Figure 8a). This observation suggests a decline in the degradation rate with increasing dye concentration, which proves the bioreactor's potential for treating diverse dyes. Due to its structural complexity, particularly the higher number of aromatic cycles in its molecule, DR227 poses a greater challenge for biological degradation compared to RB19. Aromatic rings are known to be more resistant to breakdown by biological processes. In order to enhance treatment efficiency for DR227 dye, we can optimize the residence time within the biological reactor. Residence time refers to the duration a molecule spends within a treatment system. It can be influenced by factors such as the height of the treatment bed (longer bed = longer residence time) or the flow rate of the solution passing through the

bed (slower flow rate = longer residence time). While these factors do not directly alter the inherent biodegradability of the molecule itself, optimizing residence time can improve the effectiveness of the biological treatment process. These results are in good agreement with what is generally found in the literature [47,53,54].

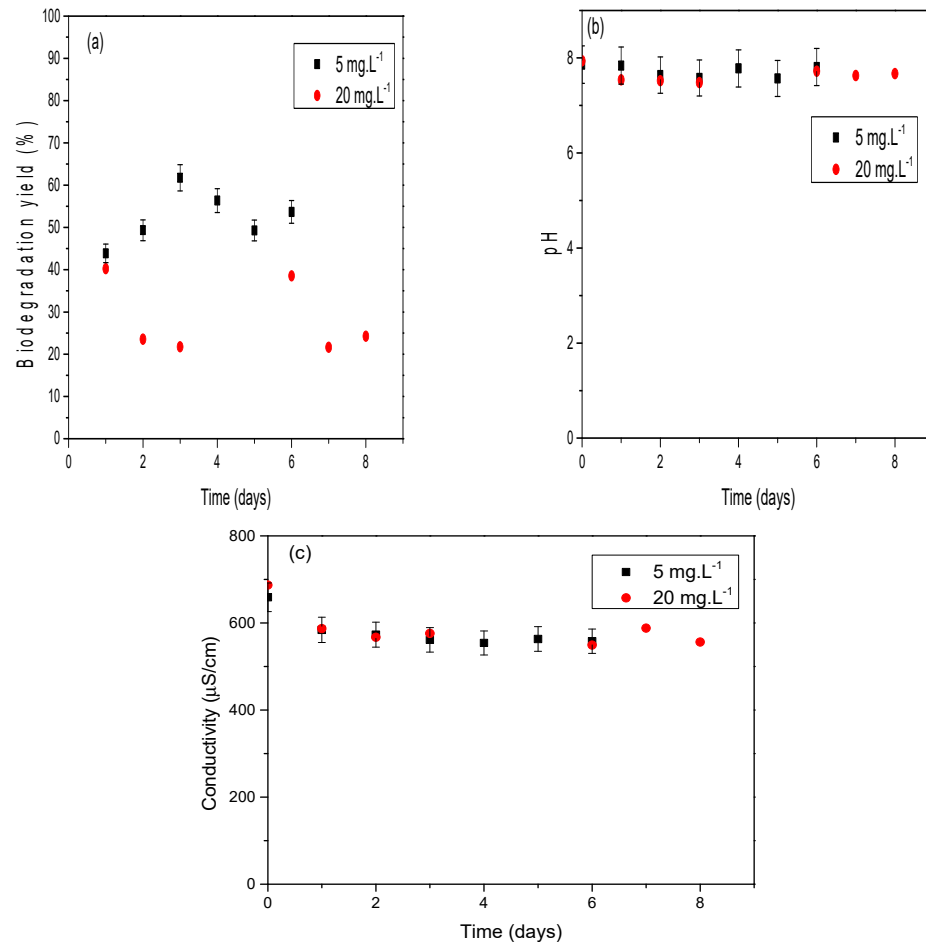


Figure 8. Effect of initial concentration of DR227. (a) Degradation yield, (b) variation of pH, (c) variation of conductivity (pH (5 mg.L⁻¹) = 8.03; pH (20 mg.L⁻¹) = 8.02; fixed bed height = 36 cm; flow rate: 0.3 L.h⁻¹).

The pH maintained a near-neutral state throughout the experiments (Figure 8b), while conductivity varied between 550 μS and 700 μS (Figure 8c).

Numerous bioreactors in continuous mode have been investigated by researchers; some of these are discussed in Table 1 [24,48,55–58].

From the previous table, we can observe that various experimental conditions were applied in the bioreactors to achieve optimal efficiency.

In this study, we explored the utilization of date pedicels, which not only served as a support for microorganisms but also act as a biostimulant, providing a rich source of nutrients. This innovative approach represents a departure from traditional supports, introducing a novel dimension to the methodology.

Table 1. Different bioreactors used in the literature.

Bioreactor Type	Substrate Material	Microorganisms	Pollutant	Experimental Conditions	Removal Rate (%)	Reference
Continuous packed bed bioreactor	Ashoka seeds	Mixed culture of microorganisms	500 mg·L ⁻¹ of Reactive Orange dye	Flow rate 1 L·h ⁻¹ For 9 days. Height of the packed bed reactor: 0.32 m	63.5	[55]
	Casuarina seeds	Mixed culture of microorganisms	500 mg·L ⁻¹ of Reactive Orange dye	Flow rate 1 L·h ⁻¹ for 9 days. Height of the packed bed reactor: 0.32 m	69.5	
Continuous packed bed bioreactor	Biochar	<i>Alcaligenes faecalis</i>	50 mg·L ⁻¹ of methylene blue (MB)	Flow rate 1.0 L·h ⁻¹ for 10 days. Height of the PBBR 10 cm loaded with 400 g of biochar.	89%	[56]
Continuous packed bed bioreactor	agar-agar	bacterial consortium EDPA containing <i>Enterobacter dissolvens</i> AGYP1 and <i>Pseudomonas aeruginosa</i> AGYP2	100 mg·L ⁻¹ of Add Maroon V	Flow rate: 15 mL·h ⁻¹ . Height of the packed bed reactor: 36 cm. Hydraulic retention time: 2.66 h.	96–97%	[57]
Continuous packed bed bioreactor	coconut shell biochar	<i>Brevibacillus parabravis</i> isolated from water bodies	500 mg·L ⁻¹ Congo red	Height of the packed bed reactor: 8 cm.	88.9%	[24]
Continuous Upflow Fixed Bed reactor	mixed support of agar and stainless-steel sponge	An effective consortium of bacteria (<i>Brevibacillus laterosporus</i>) and yeast (<i>Galactomyces geotrichum</i>)	Textile industry effluent	Flow rate: 10 mL·h ⁻¹ . Height of the fixed bed reactor: 30 cm. working volume: 182 mL.	90% decolorization of textile industry effluent and 80% reduction in COD of the effluent	[58]
Continuous up-fow packed bed bioreactor	corn-cob biochar	<i>Bacillus fexus</i> TS8, <i>Proteus mirabilis</i> PMS, and <i>Pseudomonas aeruginosa</i> NCH were carried out from the textile wastewater	500 mg·L ⁻¹ of Indanthrene Blue RS dye	Flow rate: 0.25 L·h ⁻¹ . Height of the packed bed reactor: 20 cm loaded with 400 g of CC-biochar	90%	[48]
Continuous fixed bed bioreactor	Date pedicels	<i>Activated sludge</i>	100 mg·L ⁻¹ of Reactif Bleu dye (RB19)	Flow rate: 0.3 L·h ⁻¹ . Height of the fixed bed reactor: 106.5 cm	83%	This study

3.3. Biodegradability

BOD₅ is defined by the quantity of oxygen consumed by microorganisms over 5 days to ensure the biological degradation of organic matter. This measurement provides an approximation of the load of biodegradable organic matter in a discharge. The COD/BOD₅ ratio provides a first estimate of the biodegradability of organic matter in an effluent.

A BOD₅/COD ratio equal to 0.5 indicates a biodegradable effluent [59]. The BOD₅/COD results for the initial and final treated solutions are presented in Table 2.

Table 2. BOD₅/COD results for initial and final treated solutions.

RB19 Dye Solutions mg·L ⁻¹	5 mg·L ⁻¹	20 mg·L ⁻¹	100 mg·L ⁻¹	Recycling 1	Recycling 2	5 mg·L ⁻¹ (Without Seeding)
Initial	0	0	0	0.25	0.48	0
Final	0.58	0.36	0.25	0.48	0.54	0.51

We notice an improvement in the biodegradability of solutions treated by biological purification. The solutions of the RB19 dye at a low concentration of 5 mg·L⁻¹ with and without inoculation of the culture medium became biodegradable after treatment with fixed bed since the biodegradability ratio is greater than 0.5 [48].

The biodegradability improved significantly for the RB19 dye solution with an initial concentration of $100 \text{ mg}\cdot\text{L}^{-1}$ without seeding by recycling it twice in the fixed biomass column; the BOD_5/COD ratio indicates that recycling solution 2 is biodegradable (Table 2).

Azizi et al. (2021) have evaluated the 4-chlorophenol (4-CP) removal by a mixed microbial consortium in the airlift packed bed bioreactor (ALPBB) and modeling by an artificial neural network (ANN); they found that the BOD_5/COD ratio decreased with the increase of the pollutant initial concentration from 0.96 at $1 \text{ mg}\cdot\text{L}^{-1}$ to 0.05 at $1000 \text{ mg}\cdot\text{L}^{-1}$ [60].

3.4. Phytotoxicity Test

Phytotoxicity is the ability of a compound to cause temporary or lasting damage to plants [33].

Monitoring the toxicity of dyes processed by microorganisms is essential. This ensures that the degradation products are less toxic compared to the original dyes before releasing the treated wastewater. Ideally, the treated effluent could then be considered for potential reuse in applications such as irrigation.

To evaluate the safety of these processed dyes, researchers typically assess several types of toxicity, including microbial toxicity (impact on microbial populations in the environment), genotoxicity (potential for DNA damage), cytotoxicity (effects on living cells), and phytotoxicity (impact on plant growth).

While phytotoxicity assays are commonly used due to their relative simplicity, a comprehensive safety assessment should ideally consider all these toxicity types for a complete picture.

Figure 9 illustrates the germination index using watercress (Figure 9a) and lettuce seeds (Figure 9b) to evaluate the potential negative effects of the treated dye solutions and the pure RB19 molecule on plant growth. The results were encouraging, indicating no signs of phytotoxicity for either the parent dye or its biodegradation metabolites on both seed types. This is evidenced by germination indices exceeding 80% across all tested dye solutions. In simpler terms, these findings suggest that neither the treated solutions nor the untreated pollutant exhibited toxicity towards the germination of watercress and lettuce seeds.

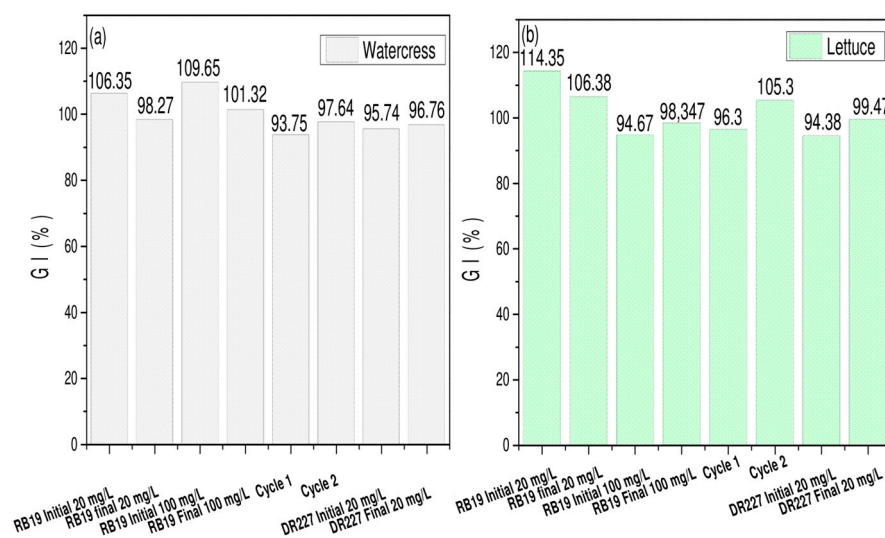


Figure 9. Germination phytotoxicity test before and after treatment (flow rate: $0.3 \text{ L}\cdot\text{h}^{-1}$). (a) Germination phytotoxicity test with watercress seeds. (b) Germination phytotoxicity test with lettuce seeds.

Adnan et al. (2015) studied the biodegradation of the dye Acid Red 27 (RA27) by the fungus strain *Armillaria* sp. F022. The evaluation of the toxicity of the degradation products was carried out by the seed berries of *Sorghum vulgare* and *Triticum aestivum* by monitoring the length of the roots. This study shows that the metabolic products of AR27 treated with *Armillaria* sp. F022 were not phytotoxic towards the two seeds used; therefore,

these products can be discharged into the wastewater network or used for agricultural purposes [61].

Tiar et al. (2018) carried out the phytotoxicity test on pepper seeds: *Capsicum annuum* commonly cultivated in the Souss Massa region. The phytotoxicity test revealed that the products generated after the biodegradation of Methyl Red (MR) dye are less toxic than the original dye [62].

3.5. Characterization of the Biological Support

3.5.1. Scanning Electron Microscopy (SEM)

The scanning electron microscopy (SEM) analysis provided valuable insights into the structure of the material. Figure 10a represents date pedicels before treatment (DPB), while Figure 10b illustrates the pedicels after treatment (DPA).

Interestingly, the material exhibited a more homogeneous structure after treatment, suggesting a better organization of its components. In contrast, the date pedicels before treatment displayed a heterogeneous structure characterized by a less uniform surface with potential variations in composition or organization.

This observed difference in structure (heterogeneous in DPB vs. homogeneous in DPA) can be attributed to the deposition of a bacterial film. Biological treatment often involves the establishment of microbial communities that break down organic matter.

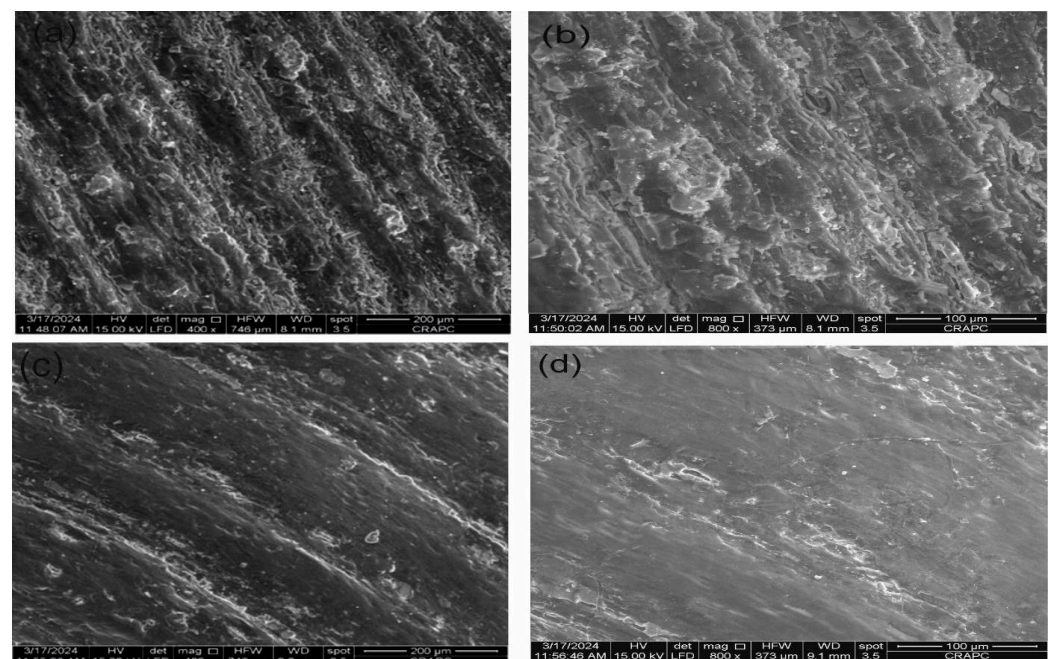


Figure 10. Scanning electron microscopy of DPB (a,b) and DPA (c,d) at different magnifications.

The accumulation of these microbes and their byproducts on the surface of the date pedicels might create a new, smoother layer, further contributing to the homogeneous appearance observed in the SEM analysis. Similar results were obtained by Yazid et al. (2011) while studying the adsorption of cadmium onto biologically treated date pedicels [36].

3.5.2. FTIR Spectra

The FTIR analysis of date pedicels was conducted to observe the chemical changes that might occur during the biodegradation process. Figure 11a represents date pedicels before biological treatment (DPB), while Figure 11b represents date pedicels after biological treatment (DPA).

The DPB spectrum, which represents the date pedicels before biological treatment, exhibited a wider range of peaks compared to the DPA spectrum. This indicates the

presence of various functional groups in the untreated pedicels. These peaks can be tentatively assigned to specific molecular vibrations as follows:

C-H stretching vibrations in aliphatic chains, observed at 2914.81 cm^{-1} and 2846.60 cm^{-1} . These absorption bands generally include contributions from cellulose, hemicellulose, and lignin [63].

C=O stretching vibrations appearing at 1734.77 cm^{-1} can be attributed to the carbonyl group of the hemicelluloses [64].

C-H bending vibrations of lignin, noted at 1461.25 cm^{-1} [65,66].

C-O stretching vibrations in cellulose and hemicellulose, seen at 1170.06 cm^{-1} and 1029.89 cm^{-1} [67].

In contrast, the DPA spectrum, representing the date pedicels after treatment, displayed fewer peaks, indicating a reduction in the variety of functional groups. Notably, a peak at 1420.70 cm^{-1} was present, which is indicative of aromatic C=C stretching vibrations [68]. This peak suggests the presence of lignin, a major component of plant cell walls. Additionally, peaks at 849.86 cm^{-1} and 711.10 cm^{-1} could potentially be attributed to C-H bending in aromatic rings of cellulose [63].

The disappearance of certain peaks in the DPA spectrum, which were present in the DPB spectrum, indicates the degradation or transformation of specific functional groups due to the biological treatment. This can be explained by the breakdown of complex polymers like lignin into simpler molecules, consumption of certain organic compounds by microorganisms, or chemical reactions altering the molecular structure of the compounds present in the date pedicels [67].

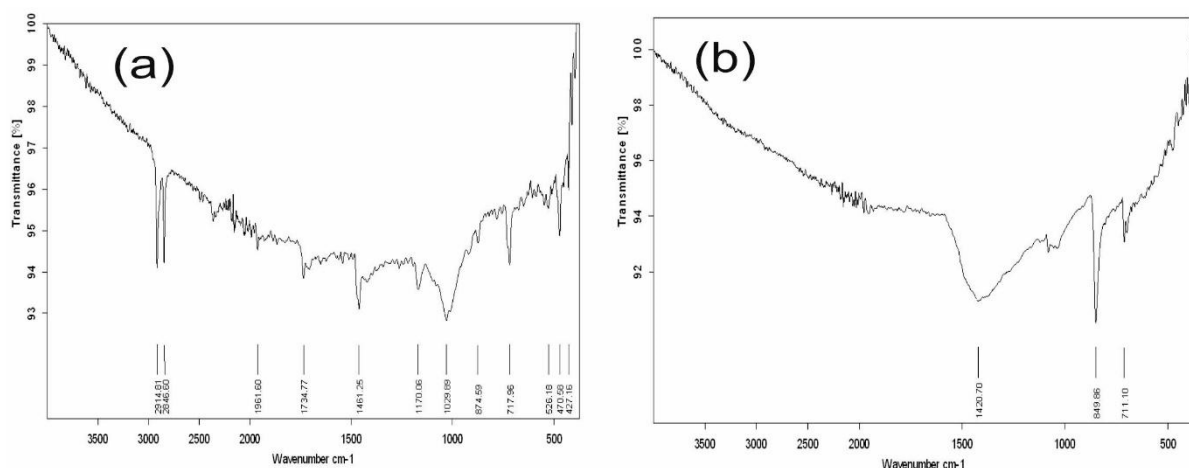


Figure 11. FTIR spectra of DPB (a) and DPA (b).

This study presents a sustainable and innovative application of date pedicels as a biological support in fixed bed reactors to address the challenge of textile dye wastewater pollution. By utilizing local agricultural waste, specifically date pedicels, this approach aligns with the principles of the circular economy. It aims to conserve raw materials and reduce energy consumption in the typically resource-intensive processes involved in wastewater treatment.

In addition to providing an eco-friendly solution for dye removal, this approach underscores the importance of engaging key stakeholders such as companies, the public, NGOs, and policymakers. These groups can play a critical role in adopting and promoting sustainable practices, such as the use of agricultural by-products in industrial processes, to meet environmental challenges. Policies aimed at fostering zero emissions or low carbon footprints, including the integration of circular economy principles, will be vital for reducing the environmental impact of wastewater treatment technologies and ensuring the conservation of natural resources [69].

Furthermore, the biological support material, after the bioremediation process, can be repurposed as an adsorbent for the removal of heavy metals, as demonstrated in the study by Yazid et al. (2011) [36]. This low-cost, eco-friendly adsorbent helps prevent secondary pollution while further supporting circular economy practices. This approach not only minimizes the carbon footprint but also promotes environmental sustainability by conserving energy and reducing waste, effectively addressing both the environmental and economic dimensions of the textile dye removal challenge.

4. Conclusions

This study explored the biodegradation of two textile dyes (RB19 and DR227) using a novel bioreactor design. The design employed a fixed bed column filled with date pedicels, acting as a support and potential biostimulant for microorganisms.

The investigation comprised two parts. The first part evaluated biodegradation with activated sludge inoculum. Here, the study revealed the impact of operational parameters on RB19 degradation. Notably, higher column heights (106.5 cm) achieved better decolorization (70%) compared to lower heights (51% at 36 cm). Interestingly, color reduction yields were similar for initial dye concentrations of 20 mg/L and 100 mg/L (around 65%), suggesting the system's tolerance to a range of dye concentrations. Furthermore, recycling the 100 mg/L RB19 solution twice through the column demonstrated the effectiveness of multiple treatment cycles.

The second part focused on biodegradation without initial inoculation. The fixed bed bioreactor spontaneously developed bacterial populations capable of degrading RB19. While the removal efficiency with seeding (70%) was slightly higher than without seeding (60%), both scenarios demonstrated the degrading ability of the established microbial community. Microscopic analysis revealed a diverse microbial community with a predominance of flocculent bacteria, coexisting with other types such as nematodes, ciliates (*Aspidisca* and *Paramecium*), and microalgae (diatoms). This diverse ecosystem likely contributes to the biodegradation process.

The bioreactor maintained a neutral pH throughout the experiment, indicating a stable operating environment for the microbial community. Conductivity fluctuated between 567 μ S and 640 μ S, potentially reflecting changes in ionic content due to dye degradation processes. Notably, the bioreactor exhibited a higher removal efficiency for DR227 at lower initial concentrations (50% at 5 mg/L vs. 20% at 20 mg/L), suggesting a concentration-dependent degradation process.

Most importantly, all treated RB19 solutions exhibited improved biodegradability, demonstrating the effectiveness of the bioreactor system in transforming these pollutants into more easily degradable compounds. Additionally, phytotoxicity tests using watercress and lettuce seeds showed no negative impact for any RB19 treated solution, indicating their environmental safety.

The characterization of dates pedicels by scanning electron microscopy (SEM) analysis revealed significant changes in the surface morphology of the date pedicels following biodegradation. Dates pedicels before treatment (DPB) exhibited a heterogeneous structure, while those after treatment (DPA) displayed a more homogeneous appearance. Furthermore, Fourier-Transform Infrared (FTIR) spectroscopy analysis highlights the significant chemical transformations that the date pedicels underwent during the biological treatment, reflecting the introduction of new functional groups and the degradation of existing ones. This work highlights the promising potential of fixed bed bioreactors with date pedicels for biodegradation of textile dyes. The results demonstrate that the established microbial community within the bioreactor can effectively degrade these pollutants, thereby reducing their environmental impact. Further research could optimize operational parameters such as flow rate and residence time within the bioreactor. Additionally, exploring the degradation of a wider range of textile dyes with varying structures is crucial for assessing the broader applicability of this technology for wastewater treatment. Overall, this study

paves the way for the development of sustainable and effective bioremediation strategies for textile wastewater.

Author Contributions: S.C.: Conceptualization, methodology, investigation, data curation, and drafting of the manuscript. H.R.-Y.: conceptualization, methodology, resources, investigation, and reviewing. S.A.: methodology, data curation, and investigation. I.T.: methodology, data curation, and investigation. N.B.: methodology. M.B.: resources. H.D.: investigation, reviewing, and submission. Z.S.: resources and investigation. All authors have read and agreed to the published version of the manuscript.

Funding: This research received no external funding.

Data Availability Statement: The original contributions presented in the study are included in the article, further inquiries can be directed to the corresponding author.

Acknowledgments: The authors would like to thank Sabra Hemidouche (Centre de Recherche Scientifique et Technique en Analyses Physico-Chimiques) for her assistance in conducting SEM and FTIR analysis.

Conflicts of Interest: The authors declare that they have no known competing financial interests or personal relationships that could have appeared to influence the work reported in this paper.

References

1. Dutta, S.; Adhikary, S.; Bhattacharya, S.; Roy, D.; Chatterjee, S.; Chakraborty, A.; Banerjee, D.; Ganguly, A.; Nanda, S.; Rajak, P. Contamination of textile dyes in aquatic environment: Adverse impacts on aquatic ecosystem and human health, and its management using bioremediation. *J. Environ. Manag.* **2024**, *353*, 120103. [\[CrossRef\]](#) [\[PubMed\]](#)
2. Saravanan, S.; Carolin, C.F.; Kumar, P.S.; Chitra, B.; Rangasamy, G. Biodegradation of textile dye Rhodamine-B by *Brevundimonas diminuta* and screening of their breakdown metabolites. *Chemosphere* **2022**, *308*, 136266. [\[CrossRef\]](#)
3. Jorge, A.M.S.; Athira, K.K.; Alves, M.B.; Gardas, R.L.; Pereira, J.F.B. Textile dyes effluents: A current scenario and the use of aqueous biphasic systems for the recovery of dyes. *J. Water Process Eng.* **2023**, *55*, 104125. [\[CrossRef\]](#)
4. Santiago, D.; Cunha, J.; Cabral, I. Chromatic and medicinal properties of six natural textile dyes: A review of eucalyptus, weld, madder, annatto, indigo and woad. *Heliyon* **2023**, *9*, e22013. [\[CrossRef\]](#) [\[PubMed\]](#)
5. Yao, H.Y.; Guo, H.; Shen, F.; Li, T.; Show, D.Y.; Ling, M.; Yan, Y.G.; Show, K.Y.; Lee, D.J. Anaerobic-aerobic treatment of high-strength and recalcitrant textile dyeing effluents. *Bioresour. Technol.* **2023**, *379*, 129060. [\[CrossRef\]](#) [\[PubMed\]](#)
6. Umesh, M.; Suresh, S.; Santosh, A.S.; Prasad, S.; Chinnathambi, A.; Al Obaid, S.; Jhanani, G.K.; Shanmugam, S. Valorization of pineapple peel waste for fungal pigment production using *Talaromyces albobiverticillius*: Insights into antibacterial, antioxidant and textile dyeing properties. *Environ. Res.* **2023**, *229*, 115973. [\[CrossRef\]](#)
7. Vaiano, V.; Sacco, O.; Libralato, G.; Lofrano, G.; Siciliano, A.; Carraturo, F.; Guida, M.; Carotenuto, M. Degradation of anionic azo dyes in aqueous solution using a continuous flow photocatalytic packed-bed reactor: Influence of water matrix and toxicity evaluation. *J. Environ. Chem. Eng.* **2020**, *8*, 104549. [\[CrossRef\]](#)
8. Mustafa, G.; Tariq Zahid, M.; Ali, S.; Zaghun Abbas, S.; Rafatullah, M. Biodegradation and discoloration of disperse blue-284 textile dye by *Klebsiella pneumoniae* GM-04 bacterial isolate. *J. King Saud Univ.-Sci.* **2021**, *33*, 101442. [\[CrossRef\]](#)
9. Tamil Selvan, S. Eco-technological approaches for textile dye effluent treatment and carbon dioxide (CO₂) capturing using green microalga *Chlorella vulgaris*. *Mater. Today Proc.* **2023**. [\[CrossRef\]](#)
10. Zehra, F.; Tyagi, N.; Mittal, H.; Kumar Singh, M.; Khanuja, M. Synthesis and comparative study of Zeolite imidazole framework for the removal of textile dyes from wastewater. *Mater. Today Proc.* **2023**. [\[CrossRef\]](#)
11. Muhamad, N.; Soontornnon Sinchai, P.; Tansom, U. Banana peel as bioremediation agent in textile dyes decolorization for wastewater management. *Biochem. Syst. Ecol.* **2023**, *106*, 104582. [\[CrossRef\]](#)
12. Wei, Y.; Zhu, Q.; Xie, W.; Wang, X.; Li, S.; Chen, Z. Biocatalytic enhancement of laccase immobilized on ZnFe₂O₄ nanoparticles and its application for degradation of textile dyes. *Chin. J. Chem. Eng.* **2024**, *68*, 216–223. [\[CrossRef\]](#)
13. Youcef, R.; Sabba, N.; Benhadji, A.; Djelal, H.; Fakhfakh, N. Nanofiltration Treatment of Industrial Wastewater Doped with Organic Dye: A Study of Hydrodynamics and Specific Energy. *Processes* **2022**, *10*, 2277. [\[CrossRef\]](#)
14. Ghaffar, A.; Mehdi, M.; Otho, A.A.; Tagar, U.; Hakro, R.A.; Hussain, S. Electrospun silk nanofibers for numerous adsorption-desorption cycles on Reactive Black 5 and reuse dye for textile coloration. *J. Environ. Chem. Eng.* **2023**, *11*, 111188. [\[CrossRef\]](#)
15. Rima, S.A.J.; Paul, G.K.; Islam, S.; Akhtar-E-Ekram, M.; Zaman, S.; Abu Saleh, M.; Salah Uddin, M. Efficacy of *Pseudomonas* sp. and *Bacillus* sp. in textile dye degradation: A combined study on molecular identification, growth optimization, and comparative degradation. *J. Hazard. Mater. Lett.* **2022**, *3*, 100068. [\[CrossRef\]](#)
16. Cui, J.; Feng, Y.; Xu, B.; Zhang, W.; Tan, L. Reactor performance of static magnetic field membrane bioreactor for treating actual high-salt textile dyeing wastewater and possible mechanism on magnetically enhanced membrane fouling control. *Process Saf. Environ. Prot.* **2023**, *179*, 835–846. [\[CrossRef\]](#)

17. Thoa, L.T.K.; Thao, T.T.P.; Nguyen-Thi, M.L.; Chung, N.D.; Ooi, C.W.; Park, S.M.; Lan, T.T.; Quang, H.T.; Khoo, K.S.; Show, P.L.; et al. Microbial biodegradation of recalcitrant synthetic dyes from textile-enriched wastewater by *Fusarium oxysporum*. *Chemosphere* **2023**, *325*, 138392. [\[CrossRef\]](#)
18. Heragy, M.O.; Moustafa, A.A.M.; Elzanfaly, E.S.; Al-Shareef, W.A.; Saad, A.S. Miniaturized solid-state sensor for inline monitoring of the microbial biodegradation of a biohazardous textile azo dye (Direct Red-81). *Talanta Open* **2022**, *6*, 100146. [\[CrossRef\]](#)
19. Herath, I.S.; Udayanga, D.; Jayasanka, D.J.; Hewawasam, C. Textile dye decolorization by white rot fungi—A review. *Bioresour. Technol. Rep.* **2024**, *25*, 101687. [\[CrossRef\]](#)
20. Huang, J.; Ling, J.; Kuang, C.; Chen, J.; Xu, Y.; Li, Y. Microbial biodegradation of aniline at low concentrations by *Pigmentiphaga daeguensis* isolated from textile dyeing sludge. *Int. Biodeterior. Biodegrad.* **2018**, *129*, 117–122. [\[CrossRef\]](#)
21. Kurade, M.B.; Waghmode, T.R.; Patil, S.M.; Jeon, B.H.; Govindwar, S.P. Monitoring the gradual biodegradation of dyes in a simulated textile effluent and development of a novel triple layered fixed bed reactor using a bacterium-yeast consortium. *Chem. Eng. J.* **2017**, *307*, 1026–1036. [\[CrossRef\]](#)
22. Srinivasan, S.; Sadasivam, S.K. Exploring docking and aerobic-microaerophilic biodegradation of textile azo dye by bacterial systems. *J. Water Process Eng.* **2018**, *22*, 180–191. [\[CrossRef\]](#)
23. Srinivasan, S.; Parameswari, M.K.; Nagaraj, S. Latest Innovations in Bacterial Degradation of Textile Azo Dyes. In *Emerging Technologies in Environmental Bioremediation*; Elsevier: Amsterdam, The Netherlands, 2020; ISBN 9780128198605.
24. Abu Talha, M.; Goswami, M.; Giri, B.S.; Sharma, A.; Rai, B.N.; Singh, R.S. Bioremediation of Congo red dye in immobilized batch and continuous packed bed bioreactor by *Brevibacillus parabrevis* using coconut shell bio-char. *Bioresour. Technol.* **2018**, *252*, 37–43. [\[CrossRef\]](#)
25. Padmanaban, V.C.; Geed, S.R.R.; Achary, A.; Singh, R.S. Kinetic studies on degradation of Reactive Red 120 dye in immobilized packed bed reactor by *Bacillus cohnii* RAPT1. *Bioresour. Technol.* **2016**, *213*, 39–43. [\[CrossRef\]](#) [\[PubMed\]](#)
26. Singh, K.; Arora, S. Removal of synthetic textile dyes from wastewaters: A critical review on present treatment technologies. *Crit. Rev. Environ. Sci. Technol.* **2011**, *41*, 807–878. [\[CrossRef\]](#)
27. Kureel, M.K.; Geed, S.R.; Rai, B.N.; Singh, R.S. Novel investigation of the performance of continuous packed bed bioreactor (CPBBR) by isolated *Bacillus* sp. M4 and proteomic study. *Bioresour. Technol.* **2018**, *266*, 335–342. [\[CrossRef\]](#)
28. Cherif, S.; Rezzaz-Yazid, H.; Sadaoui, Z.; Trari, M. Biodegradation of Remazol Blue Brilliant R Dye Using Date Pedicels as a Biostimulant. *J. Water Chem. Technol.* **2021**, *43*, 164–172. [\[CrossRef\]](#)
29. Allalou, O.; Miroud, D.; Belmedani, M.; Sadaoui, Z. Performance of surfactant-modified activated carbon prepared from dates wastes for nitrate removal from aqueous solutions. *Environ. Prog. Sustain. Energy* **2019**, *38*, S403–S411. [\[CrossRef\]](#)
30. Chandrasekhar, K.; Mehrez, I.; Kumar, G.; Kim, S. Relative evaluation of acid, alkali, and hydrothermal pretreatment influence on biochemical methane potential of date biomass. *J. Environ. Chem. Eng.* **2021**, *9*, 106031. [\[CrossRef\]](#)
31. Shokrollahi, S.; Denayer, J.F.M.; Karimi, K. Efficient bioenergy recovery from different date palm industrial wastes. *Energy* **2023**, *272*, 127057. [\[CrossRef\]](#)
32. Yazid, H.; Hammadi, W.; Selama, A. *Etude de la Dénitrification Biologique des Eaux Polluées par les Nitrates en Utilisant les Pédicelles de Dattes Comme Support et Substrat Organique Pour la Microflore Dénitrifiante*; SFGP: Paris, France, 2013; pp. 1–8.
33. Cherif, S.; Djelal, H.; Firmin, S.; Bonnet, P.; Frezet, L.; Kane, A.; Amine Assadi, A.; Trari, M.; Yazid, H. The impact of material design on the photocatalytic removal efficiency and toxicity of two textile dyes. *Environ. Sci. Pollut. Res.* **2022**, *29*, 66640–66658. [\[CrossRef\]](#) [\[PubMed\]](#)
34. Cherif, S.; Bonnet, P.; Frezet, L.; Kane, A.; Assadi, A.A.; Trari, M.; Yazid, H. The photocatalytic degradation of a binary textile dyes mixture within a new configuration of loop reactor using ZnO thin film-phytotoxicity control. *Comptes Rendus Chim.* **2022**, *25*, 1–19. [\[CrossRef\]](#)
35. Cherif, S.; Yazid, H.; Rekhila, G.; Sadaoui, Z.; Trari, M. Optik The optical and photo-electrochemical characterization of nano-ZnO particles and its application to degradation of Reactive Blue 19 under solar light. *Optik* **2021**, *238*, 166751. [\[CrossRef\]](#)
36. Yazid, H.; Sadaoui, Z.; Maachi, R. Removal of cadmium (II) ions from aqueous phase by biosorption on biological activated dates' pedicels (kinetic, equilibrium and thermodynamic study). *Int. J. Chem. React. Eng.* **2011**, *9*. [\[CrossRef\]](#)
37. Picard, C.; Logette, S.; Schrotter, J.C.; Aimar, P.; Remigy, J.C. Mass transfer in a membrane aerated biofilm. *Water Res.* **2012**, *46*, 4761–4769. [\[CrossRef\]](#) [\[PubMed\]](#)
38. Emanuelsson, E.A.C.; Livingston, A.G. Overcoming oxygen limitations in membrane-attached biofilms—Investigation of flux and diffusivity in an anoxic biofilm. *Water Res.* **2004**, *38*, 1530–1541. [\[CrossRef\]](#) [\[PubMed\]](#)
39. Moussavi, G.; Ghorbanian, M. The biodegradation of petroleum hydrocarbons in an upflow sludge-blanket / fixed-film hybrid bioreactor under nitrate-reducing conditions: Performance evaluation and microbial identification. *Chem. Eng. J.* **2015**, *280*, 121–131. [\[CrossRef\]](#)
40. Ghorbanian, M.; Moussavi, G.; Farzadkia, M. International Biodeterioration & Biodegradation Investigating the performance of an up-flow anoxic fixed-bed bioreactor and a sequencing anoxic batch reactor for the biodegradation of hydrocarbons in petroleum-contaminated saline water. *Int. Biodeterior. Biodegrad.* **2014**, *90*, 106–114. [\[CrossRef\]](#)
41. Alam, R.; Ardiati, F.C.; Solihat, N.N.; Alam, M.B.; Lee, S.H.; Yanto, D.H.Y.; Watanabe, T.; Kim, S. Biodegradation and metabolic pathway of anthraquinone dyes by *Trametes hirsuta* D7 immobilized in light expanded clay aggregate and cytotoxicity assessment. *J. Hazard. Mater.* **2020**, *405*, 124176. [\[CrossRef\]](#)

42. Mohammed, I.; Bala, U.; Hussaini, A.; Saleh, D.; Aliyu, M.; Noor, A.; Haruna, A.; Hussaini, A. Case Studies in Chemical and Environmental Engineering Sequential batch reactors for aerobic and anaerobic dye removal: A mini-review. *Case Stud. Chem. Environ. Eng.* **2023**, *8*, 100547. [[CrossRef](#)]
43. Robinson, T.; McMullan, G.; Marchant, R.; Nigam, P. Remediation of dyes in textile effluent: A critical review on current treatment technologies with a proposed alternative. *Bioresour. Technol.* **2001**, *77*, 247–255. [[CrossRef](#)] [[PubMed](#)]
44. Enayatzamir, K.; Alikhani, H.A.; Rodríguez, S. Simultaneous production of laccase and decolouration of the diazo dye Reactive Black 5 in a fixed-bed bioreactor. *J. Hazard. Mater.* **2009**, *164*, 296–300. [[CrossRef](#)] [[PubMed](#)]
45. El Jaafari, A.; Boutaleb, N.; Bahlaouan, B.; Aitcheikh, A.; Taiek, T.; Jada, A.; Lazar, S.; Antri, S. El Biodegradation of Dairy Wastewater by the Use of Fish Scales as Packing in Moving Bed Bioreactors. *J. Colloid Sci. Biotechnol.* **2017**, *5*, 218–222. [[CrossRef](#)]
46. Boeglin, J.-C. Traitements biologiques des eaux résiduaires. *Procédés Chim.-Bio-Agro Bioprocédés Bioprod.* **1998**, *J3942*, 28. [[CrossRef](#)]
47. Tiwari, H.; Kumar, R.; Sharan, R. Bioresource Technology A comprehensive evaluation of the integrated photocatalytic-fixed bed bioreactor system for the treatment of Acid Blue 113 dye. *Bioresour. Technol.* **2022**, *364*, 128037. [[CrossRef](#)]
48. Mohanty, S.S.; Kumar, A. Biodegradation of Indanthrene Blue RS dye in immobilized continuous upflow packed bed bioreactor using corncob biochar. *Sci. Rep.* **2021**, *11*, 13390. [[CrossRef](#)] [[PubMed](#)]
49. Hamaidi-Chergui, F.; Zoubiri, A.; Debib, A.; Hamaidi, M.; Kais, H. Evaluation de la charge en pathogènes et de la microfaune dans les eaux de l'effluent brute et traité rejeté dans un milieu récepteur: Cas de la station d'épuration de Médéa. *Larhyss J.* **2016**, *26*, 183–208.
50. Canler, J.-P.; Perret, J.-M.; Duchène, P.; Cotteux, É. *Aide au Diagnostic des Stations D'épuration par L'observation Microscopique des Boues Activées*; Cemagref: Lyon, France, 1999.
51. Hatam-nahavandi, K.; Mahvi, A.H.; Mohebbi, M.; Keshavarz, H.; Mobedi, I. Environmental Health Detection of parasitic particles in domestic and urban wastewaters and assessment of removal efficiency of treatment plants in Tehran, Iran. *J. Environ. Health Sci. Eng.* **2015**, *13*, 1–13. [[CrossRef](#)]
52. Khaldi, H. Étude de Possibilité D'épuration des Eaux Usées par un Mélange Boues-Micro-Algues. Cas de la Station D'épuration de Tiaret (Algérie). Ph.D. Thesis, Université Ibn Khaldoune, Tiaret, Algeria, 2018.
53. Al-zawahreh, K.; Teresa, M.; Al-degs, Y. Environmental Technology & Innovation Competitive removal of textile dyes from solution by pine bark-compost in batch and fixed bed column experiments. *Environ. Technol. Innov.* **2022**, *27*, 102421. [[CrossRef](#)]
54. Kulkarni, A.N.; Watharkar, A.D.; Rane, N.R.; Jeon, B. Ecotoxicology and Environmental Safety Decolorization and detoxification of dye mixture and textile effluent by lichen *Dermatocarpon vellereceum* in fixed bed up flow bioreactor with subsequent oxidative stress study. *Ecotoxicol. Environ. Saf.* **2018**, *148*, 17–25. [[CrossRef](#)]
55. Bharti, V.; Shahi, A.; Geed, S.R.; Kureel, M.K.; Rai, B.N.; Kumar, S.; Giri, B.S.; Singh, R.S. Biodegradation of reactive orange 16 (RO-16) dye in packed bed bioreactor using seeds of Ashoka and Casuarina as packing medium. *Indian J. Biotechnol.* **2017**, *16*, 216–221.
56. Bharti, V.; Vikrant, K.; Goswami, M.; Tiwari, H.; Sonwani, R.K.; Lee, J.; Tsang, D.C.W.; Kim, K.H.; Saeed, M.; Kumar, S.; et al. Biodegradation of methylene blue dye in a batch and continuous mode using biochar as packing media. *Environ. Res.* **2019**, *171*, 356–364. [[CrossRef](#)] [[PubMed](#)]
57. Patel, Y.; Gupte, A. Biological Treatment of Textile Dyes by Agar-Agar Immobilized Consortium in a Packed Bed Reactor. *Water Environ. Res.* **2015**, *87*, 242–251. [[CrossRef](#)]
58. Kurade, M.B.; Waghmode, T.R.; Xiong, J.Q.; Govindwar, S.P.; Jeon, B.H. Decolorization of textile industry effluent using immobilized consortium cells in upflow fixed bed reactor. *J. Clean. Prod.* **2019**, *213*, 884–891. [[CrossRef](#)]
59. Zeghioud, H.; Khellaf, N.; Amrane, A.; Djelal, H.; Bouhelassa, M.; Assadi, A.A.; Rtimi, S. Combining photocatalytic process and biological treatment for Reactive Green 12 degradation: Optimization, mineralization, and phytotoxicity with seed germination. *Environ. Sci. Pollut. Res.* **2020**, *28*, 12490–12499. [[CrossRef](#)]
60. Azizi, E.; Abbasi, F.; Baghapour, M.A.; Shirdareh, M.R.; Shooshtarian, M.R. 4-Chlorophenol Removal By Air Lift Packed Bed Bioreactor and Its Modeling By Kinetics and Numerical Model (Artificial Neural Network). *Sci. Rep.* **2021**, *11*, 670. [[CrossRef](#)]
61. Adnan, L.A.; Hadibarata, T.; Sathishkumar, P.; Yusoff, A.R.M. Biodegradation Pathway of Acid Red 27 by White- Rot Fungus *Armillaria* sp. F022 and Phytotoxicity Evaluation. *Soil Air Water* **2016**, *44*, 239–246. [[CrossRef](#)]
62. Tiar, A.; Askarne, L.; Ait Addi, E.; Assabbane, A.; Boubaker, H. Etude de la biodégradation des polluants industriels—cas des colorants azoïques. *SMETox J.* **2018**, *1*, 63–68.
63. Nabili, A.; Fattoum, A.; Passas, R.; Elaloui, E.; Nabili, A. Extraction and Characterization of Cellulose from Date Palm Seeds (*Phoenix dactylifera* L.) Laboratory of Pulp, Paper and Graphic Arts Sciences, UMR CNRS 5518. *Cellul. Chem. Technol.* **2014**, *50*, 9–10.
64. Rocha, G.J.M.; Andrade, L.P.; Martín, C.; Araujo, G.T.; Mouchrek Filho, V.E.; Curvelo, A.A.S. Simultaneous obtaining of oxidized lignin and cellulosic pulp from steam-exploded sugarcane bagasse. *Ind. Crop. Prod.* **2020**, *147*, 112227. [[CrossRef](#)]
65. Ventura-Cruz, S.; Flores-Alamo, N.; Tecante, A. Preparation of microcrystalline cellulose from residual Rose stems (*Rosa* spp.) by successive delignification with alkaline hydrogen peroxide. *Int. J. Biol. Macromol.* **2020**, *155*, 324–329. [[CrossRef](#)] [[PubMed](#)]
66. Akhtar, A.; Ivanova, T.; Jiříček, I.; Krepl, V. Detailed characterization of waste from date palm (*Phoenix dactylifera*) branches for energy production: Comparative evaluation of heavy metals concentration. *J. Renew. Sustain. Energy* **2019**, *11*, 013102. [[CrossRef](#)]

-
67. Djaafri, M.; Drissi, A.; Mehdaoui, S.; Kalloum, S.; Atelge, M.R.; Khelafi, M.; Kaidi, K.; Salem, F.; Tahri, A.; Atabani, A.E.; et al. Anaerobic digestion of dry palms from five cultivars of Algerian date palm (*Phoenix dactylifera* L.) namely H'mira, Teggaza, Tinacer, Aghamou and Takarbouchet: A new comparative study. *Energy* **2023**, *269*, 126774. [\[CrossRef\]](#)
 68. Gatt, E. Etude de la Déconstruction de Résidus Agricoles Lignocellulosiques par Extrusion Biocatalytique. Ph.D. Thesis, Institut National Polytechnique de Toulouse, Toulouse, France, 2019.
 69. Streimikiene, D.; Kyriakopoulos, G.L. Energy Poverty and Low Carbon Energy Transition. *Energies* **2023**, *16*, 610. [\[CrossRef\]](#)

Disclaimer/Publisher's Note: The statements, opinions and data contained in all publications are solely those of the individual author(s) and contributor(s) and not of MDPI and/or the editor(s). MDPI and/or the editor(s) disclaim responsibility for any injury to people or property resulting from any ideas, methods, instructions or products referred to in the content.